Synthesis and Properties of a New Range of Mixed-Donor Alkynyl Ferrocenophanes

Anthony D. Woods,*,† German Alcalde,† Vladimir B. Golovko,† Catherine M. Halliwell,‡ Martin J. Mays,† and Jeremy M. Rawson†

Department of Chemistry, University of Cambridge, Lensfield Road, Cambridge, CB2 1EW, U.K., and National Physical Laboratory, Queens Road, Teddington, Middlesex, TW11 0LW, U.K.

Received July 15, 2004

The acid-catalyzed reaction of [1,1′-Fc{$Co_2(CO)_6(\mu{:}\eta^2$-C≡$CCMe_2OH)$}$_2$] (Fc = Fe(η^5-C_5H_4)$_2$) with a variety of dinucleophiles led to the formation in excellent yields of a novel range of ferrocenophanes containing a variety of donor atoms. The crystal structures of four of these new compounds are reported as well as the results of electrochemical studies of the new complexes.

Introduction

There is intense current interest in the synthesis and behavior of thio-macrocycles.[1−3] These compounds may be suitable for a diverse range of applications, from molecular sensors to bio-inorganic hosts.[4−7] The cyclic nature of the macrocycle limits the conformational modes available to any guest metal[8] and also makes possible the stabilization of unusual oxidation states;[9] a great deal of attention has been focused on methods to tailor macrocycles to allow them to bind specific ions.[10] This field has now been extended to include the synthesis of complexes that contain mixed-donor functionalities.[11−14] Such complexes, especially those containing both hard and soft donor atoms, are of immense interest since they can potentially bind two metals of differing character and oxidation state within the same cavity.[15]

To be able to observe the binding of guest ions, it is usual to have either a redox or chromogenic response on binding.[16] Frequently the receptor is a ferrocene-based system, although cobaltacinium and transition metal-bipyridyl systems are also well documented.[17] To attain the best communication in the host−guest complexes, it is preferable to have the donor atoms of the chelating unit directly bonded to the ferrocene.[18] It has previously been demonstrated that Nicholas reactions of cobalt-coordinated bispropargyl alcohols with dinucleophiles may yield monomeric or dimeric products depending on both the choice of nucleophile and the concentration of the reactant.[19] Thus, it was hypothesized that the use of a Nicholas reaction of dithiols with 1,1′-bispropargylferrocenes would yield interesting new ferrocenophanes containing one or two ferrocene units.

Results and Discussion

The synthetic strategy employed requires the use of 1,1′-bispropargylferrocenes, [1,1′-Fc(C≡$CR_2OH)_2$], as the key starting materials. There are few examples of 1,1′-functionalized alkynylferrocenes within the literature and, to the authors' knowledge, only one example of a 1,1′-bispropargylferrocene, [Fc(C≡$CCMe_2OH)_2$], which was synthesized in low yield by the reaction of [$FcLi_2$] with IC≡CMe_2OH and CuBr·SMe_2.[20] It was decided to use a Sonogashira type coupling to synthesize the target molecules [Fc(C≡$CCR_2OH)_2$] (R = H, Me).[21] Accordingly, 1,1′-FcI_2 was refluxed with excess HC≡CCH_2OH in Et_2-

* To whom correspondence should be addressed. E-mail: anthony_woods@ici.com.
† University of Cambridge.
‡ National Physical Laboratory.

(1) Blake, A. J.; Schröder, M. *Adv. Inorg. Chem.* **1990**, *35*, 1.
(2) Cooper, S. R. *Acc. Chem. Res.* **1988**, *21*, 141.
(3) Blake, A. J.; Li, W.-S.; Lippolis, V.; Taylor, A.; Schröder, M. *J. Chem. Soc., Dalton Trans.* **1998**, 2931.
(4) Izatt, R. M.; Pawlak, K.; Bradshaw J. S.; Breuning, R. L. *Chem. Rev.* **1991**, *91*, 1721.
(5) Smith, R. J.; Adams, G. D.; Richardson, A. P.; Küppers, H. J.; Blower, P. J. *Chem. Commun.* **1991**, 475.
(6) Blake, A. J.; Reid, G.; Schröder, M. *J. Chem. Soc., Dalton Trans.* **1990**, 3849.
(7) Neve, F.; Ghedini, M.; Francescangeil, M. *Liq. Cryst.* **1996**, *21,* 625.
(8) Lindoy, L. F. *The Chemistry of Macrocyclic Ligand Complexes*; Cambridge University Press: Cambridge, 1989.
(9) Blake, A. J.; Taylor, A.; Schröder, M. *Chem. Commun.* **1993**, 1097.
(10) See for example: Lindoy, L. F. *Pure Appl. Chem.* **1997**, *69*, 2179, and references therein.
(11) Danks, J. P.; Champness, N. R.; Schröder, M. *Coord. Chem. Rev.* **1998**, *174*, 417.
(12) Caltagirone, C.; Bencini, A.; Demartin, F.; Devillanova, F. A.; Garau, A.; Isaia, F.; Lippolis, V.; Mariani, P.; Papke, U.; Tei, L.; Verani, G. *J. Chem. Soc., Dalton Trans*. **2003**, 901.
(13) Fenton, R. R.; Gauci, R.; Junk, P. C.; Lindoy, L. F.; Luckay, R. C.; Meehan, G. V.; Price, J. R.; Turner, P.; Wei, G. *J. Chem. Soc., Dalton Trans*. **2002**, 2185.
(14) van de Water, L. G. A.; Buihs, W.; Driessen, W. L.; Reedijk, J. *New J. Chem.* **2001**, *25*, 243.
(15) Lucas, C. R.; Liang, W.; Miller, D. O.; Brisdon, J. N. *Inorg. Chem.* **1997**, *36*, 4508.
(16) Beer, P. D.; Gale, P. A.; Chen, G. Z. *J. Chem. Soc., Dalton Trans.* **1999**, 1897.
(17) For a recent review see: Beer, P. D.; Hayes, E. J. *Coord. Chem. Rev.* **2003**, *240*, 167.
(18) (a) Plenio, H.; Aberle, C. *Organometallics* **1997**, *16*, 5950. (b) Plenio, H.; Yang, J.; Diodane, R.; Heinze, J. *Inorg. Chem.* **1994**, *33*, 4098.
(19) (a) Hope-Weeks, L. J.; Mays, M. J.; Woods, A. D. *J. Chem. Soc., Dalton Trans.* **2002**, 1812. (b) Gibe, R.; Green, J. R. *Chem. Commun.* **2002**, 1550.
(20) Buchmeiser, M.; Schottenberger, H. *J. Organomet. Chem*. **1992**, *436*, 223.
(21) Long, N. J.; Martin, A. J.; Vilar, R.; White, A. J. P.; Williams, D. J.; Younus M. *Organometallics* **1999**, *4261*, 1. (b) Bunz, U. H. F. *Chem. Rev.* **2000**, *100*, 1605.

10.1021/om049465e CCC: $30.25
Publication on Web 01/08/2005

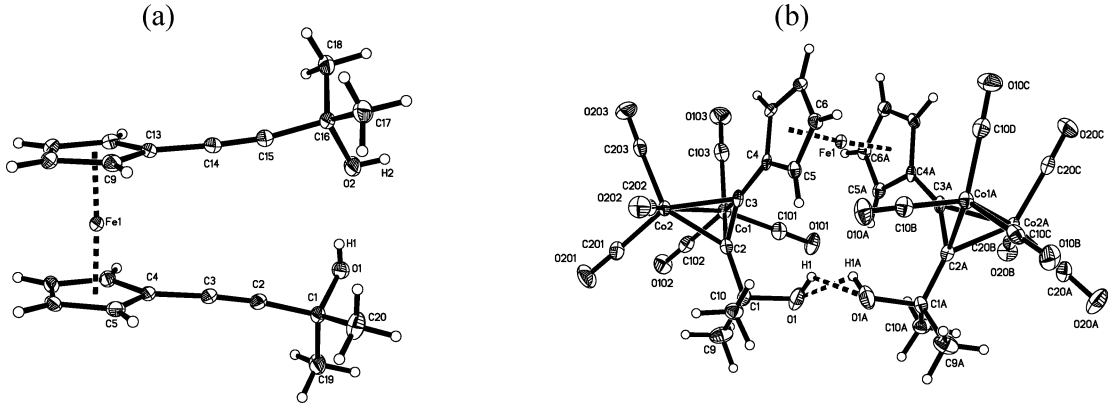

Figure 1. Molecular structure of (a) **2** and (b) **4** (ORTEP to 30% probability).

Scheme 1. Reaction of FcI_2 with Propargyl Alcohols

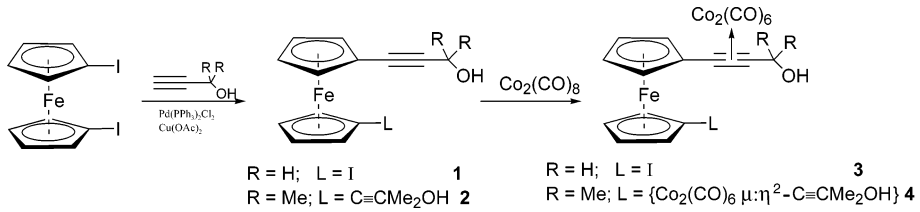

NH (which we have previously found gives the highest yield for Sonogashira couplings involving $HC{\equiv}CH_2OH$) using 1 mol % of both $Pd(PPh_3)_2Cl_2$ and CuI as catalysts. Surprisingly, despite prolonged periods of reflux and an increase in the mol % of catalyst used, no [Fc($C{\equiv}CCH_2OH)_2$] was isolated. Instead, [Fc($C{\equiv}CCH_2OH$)I] (**1**) was isolated in good (61%) yield (Scheme 1). Attempts to gain access to the target compound by the isolation of **1** followed by reaction of **1** with fresh $HC{\equiv}CCH_2OH$ under standard coupling conditions proved unsuccessful. By contrast, the reaction of FcI_2 with $HC{\equiv}CCMe_2OH$ under Sonogashira conditions did yield the desired [1,1′-Fc($C{\equiv}CCMe_2OH)_2$] (**2**) in good yield. It was found that best yields were obtained using $^iPr_2NH$ as solvent and Cu($OAc)_2$ as the cocatalyst. The yields of **2** proved significantly better than those of the previously reported synthesis, and the current synthetic strategy also proved markedly simpler, giving access to multigram quantities of **2** from readily available FcI_2.

To activate the propargyl alcohol toward nucleophilic substitution, it is first necessary to coordinate the alkyne to $Co_2(CO)_6$ (or other dicobalt fragments);[22] the positive charge of the intermediate from S_N1 substitution of the OH group is stabilized by interaction with the filled Co $d_{x^2-y^2}$ orbital.[23] Toluene solutions of compounds **1** and **2** were therefore treated with 1.1 and 2.2 equiv of $Co_2(CO)_8$, respectively. After stirring for 3 h the cobalt-complexed alkynes were isolated by flash chromatography to yield green oily [1,1′-Fc{$Co_2(CO)_6(\mu$-η^2-$C{\equiv}CCH_2OH)$}I] (**3**) and green crystalline [1,1′-Fc{Co_2-$(CO)_6(\mu$-η^2-$C{\equiv}CCMe_2OH)\}_2$] (**4**) (Scheme 1). Compounds **1**−**4** have been fully characterized by IR and ^1H and ^{13}C NMR spectroscopy as well as by LSIMS. The ^1H NMR spectrum of **1** quite clearly indicates that the two cyclopentadienyl rings are asymmetrically substituted; four triplets are observed at 4.40, 4.38, 4.20, and 4.19 ppm in the ^1H NMR spectrum of **1**. Coordination of **1** to $Co_2(CO)_6$ leads to a marked downfield shift in the propargylic CH_2 resonance from 4.41 ppm in **1** to 5.04 ppm in **3**. This downfield shift is also apparent in the ^{13}C NMR spectra of **1** and **3**, with the C≡C*C* resonance being observed at 51.09 and 63.90 ppm, respectively. The spectroscopic data for **2** are in accordance with the literature values.[20] Again, coordination of the alkyne fragment in **2** to $Co_2(CO)_6$ leads to a downfield shift in the propargylic carbon resonance from 65.66 ppm in **2** to 73.19 ppm in **4**.

Additionally, compounds **2** and **4** have been the subject of single-crystal X-ray diffraction studies (Figure 1); relevant bond lengths and angles are given in Table 1.

As is common for bis-substituted ferrocenes, the cyclopentadienyl rings of **2** are eclipsed (twist = 3.7°).[24] Unusually, however, the rings adopt a 1,1′ conformation (γ = 3.8°); the presence of a hydrogen bond between H(1) and O(2) of the two $C{\equiv}CCMe_2OH$ side chains [H(1)···O(2) 2.076 Å] presumably accounts for the adoption of this sterically disfavored geometry. The cyclopentadienyl rings are virtually planar (max. deviation 0.0038 Å) and are slightly titlted (3.4°). A further hydrogen-bonding interaction leads to the formation of a centrosymmetric dimer (Figure 2) [O(1)···H(2A) 2.117 Å] (Figure 2).

The molecular structure of **4** contains a mirror plane that passes through Fe(1). Complexation of the triple bond leads to the expected lengthening of the C(2)−C(3) bond from 1.191(3) Å in **2** to 1.345(6) Å in **4**. The cyclopentadienyl rings of **4** adopt a relative 1,3′ disposition (γ = 102.2°) and are in an unusual staggered configuration (twist = 29.88°).[24] This conformation is presumably adopted to avoid steric repulsion between the bulky $Co_2(CO)_6$ fragments and allows the formation of an intramolecular hydrogen bond [O(1)···H(1A) 2.282

(22) Nicholas, K. M.; Petit, R. *Tetrahedron Lett.* **1971**, *37*, 3475.
(23) Pfletschinger, A.; Koch, W.; Schmalz, H.-G. *Chem. Eur. J.* **2001**, 5325.
(24) Grossel, M. C.; Goldspink, M. R.; Hrihac, J. A.; Weston, S. C. *Organometallics* **1991**, *10*, 851.

Table 1. Selected Bond Lengths (Å) and Angles (deg) for 2 and 4

compound **2**		compound **4**	
mean Fe−C(5−8)	2.049	mean Fe−C(5−8)	2.046
range Fe−C(5−8)	2.043(2)−2.052(2)	range Fe−C(5−8)	2.042(2)−2.050(4)
Fe−C(4)	2.063(2)	Fe−C(4)	2.066(4)
mean Fe−C(9−12)	2.045		
range Fe−(C9−12)	2.039(2)−2.054(2)		
Fe−C(13)	2.060(2)		
C(1)−C(2)	1.481(2)	C(1)−C(2)	1.500(6)
C(2)−C(3)	1.191(3)	C(2)−C(3)	1.345(6)
C(3)−C(4)	1.431(3)	C(3)−C(4)	1.452(6)
C(13)−C(14)	1.431(3)	Co(1)−Co(2)	2.4654(9)
C(14)−C(15)	1.191(3)	Co(1)−C(2)	1.976(4)
C(15)−C(16)	1.481(3)	Co(1)−C(3)	1.967(4)
		Co(2)−C(2)	1.962(4)
		Co(2)−C(3)	1.993(4)
C(1)−C(2)−C(3)	174.0(2)	C(1)−C(2)−C(3)	140.5(3)
C(2)−C(3)−C(4)	175.4(2)	C(2)−C(3)−C(4)	146.0(4)
C(13)−C(14)−C(15)	176.5(2)		
C(14)−C(15)−C(16)	172.1(2)		

Å]. In this case, however, there are no intermolecular hydrogen bonds present, presumably because of the changed geometry of the propargylic fragments leading to steric hindrance at the O−H groups. The cyclopentadienyl rings are planar (max. deviation 0.0027 Å) and lie at an angle of 4.1° to each other. Coordination of the alkyne to $Co_2(CO)_6$ leads to the expected decrease in the alkyne *bend-back* angle [C(3)−C(2)−C(1) 140.5(3)°], which has the effect of sterically shielding O(1) by the C(9) and C(10) Me groups and preventing close approach of another molecule of **4**.[25] Notably, the bend-back angle at the ferrocene-substituted terminus is decreased by a smaller amount [C(4)−C(3)−C(2) 146.0(4)° in **4**, cf. C(4)−C(3)−C(2) 175.4(2)° in **2**] than that at the other terminus. This is presumably a consequence of competition for the alkyne's electron density between the ferrocene and the dicobalt unit. The hydrogen bond present in **4** does result in the $Co_2(CO)_6$ fragments adopting a *cisoid* configuration rather than the usual *transoid* geometry. There are no unusual features within the Co_2C_2 core of **4**.[25]

Reactions of 3. Despite the fact that **3** was not substituted by a $C{\equiv}CCH_2OH$ group at both cyclopentadienyl rings (a necessary prerequisite to the formation of ferrocenophanes), it was decided to explore the reactivity of **3** toward a variety of dithiols under acid catalysis conditions. Accordingly, a dichloromethane solution of **3** was treated with $(HSC_2H_4)_2O$ and a few drops of HBF_4 at −78 °C. Separation by preparative TLC yielded green [1,1′-Fc{$Co_2(CO)_6(\mu{:}\eta^2$-C≡CCH_2-$SC_2H_4OC_2H_4SH$)}I] (**5**) together with several minor fractions (Scheme 2). Separation of **5** proved somewhat problematic, with a good deal of decomposition occurring on the plates. To combat this, it was decided to first

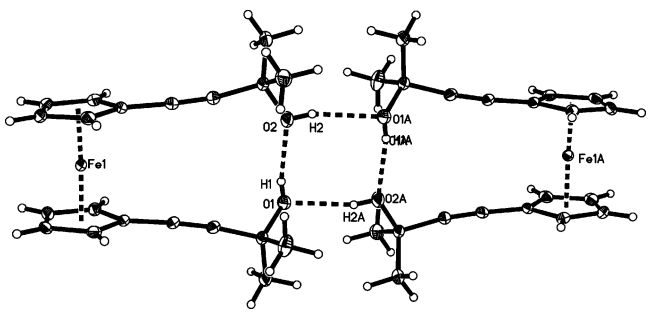

Figure 2. Hydrogen bonding within the solid-state structure of **2** (ORTEP to 30% probability).

Scheme 2. Reaction of 3 with $(HSC_2H_4)_2O$

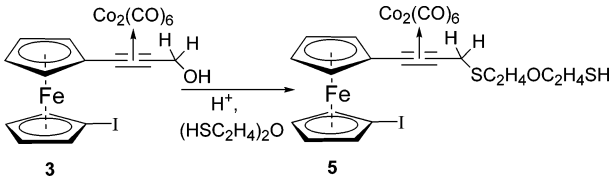

Scheme 3. Reaction of 4 with Dithiols

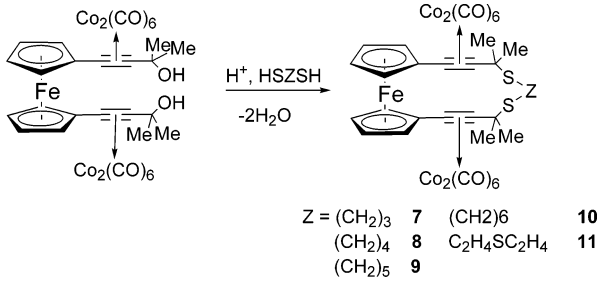

treat **3** with dppm (bis-diphenylphosphino methane); it was hoped that the dppm group might add extra stability to any products formed from the above substitution reactions. Treatment of a toluene solution of **3** with dppm at 70 °C for 2 h yielded, after chromatographic separation, red crystalline [1,1′-Fc{$Co_2(CO)_4$-(dppm)($\mu{:}\eta^2$-C≡CCH_2OH)}I] (**6**) in good yield. Unfortunately, however, the dppm unit did not help to improve the stability of any products resulting from acid-catalyzed substitution reactions.

Reactions of 4. Treatment of **4** with dithiols under acid-catalyzed reaction conditions proved appreciably more successful than the corresponding reactions of **3** or **6**. Thus treatment of **4** with the dithiols $HS(CH_2)_n$-SH (n = 3−6) and $(HSC_2H_4)_2S$ led in each case to the formation of the desired ferrocenophane [1,1′-Fc{(Co_2-$(CO)_6)_2(\mu{:}\eta^2{-}\mu{:}\eta^2$-C≡$CCMe_2S(CH_2)_nSCMe_2C{\equiv}C$)}] ($n$ = 3, **7**; n = 4, **8**; n = 5, **9**; n = 6, **10**) and [1,1′-Fc{(Co_2-$(CO)_6)_2(\mu{:}\eta^2{-}\mu{:}\eta^2$-C≡$CCMe_2SC_2H_4SC_2H_4SCMe_2C{\equiv}C$)}] (**11**) (Scheme 3). On no occasion were any dimeric compounds containing two ferrocene units isolated.

Complexes **7**−**11** have been fully characterized by IR, ^1H and ^{13}C NMR, and LSIMS. In addition, compounds **7** and **11** have been the subject of single-crystal X-ray diffraction studies (Figures 3, 4); relevant bond lengths

(25) Went, M. J. *Adv. Oragnomet. Chem.* **1997**, *41*, 69.

Table 2. Selected Bond Lengths (Å) and Angles (deg) for 7 and 11

	7	11		7	11
Co(1)−Co(2)	2.445(2)	2.4481(5)	C(1)−C(2)	1.503(9)	1.515(4)
Co(3)−Co(4)	2.472(1)	2.4659(5)	C(2)−C(3)	1.344(9)	1.340(6)
Fe−C(4)	2.071(6)	2.059(3)	Fe−C(13)	2.066(6)	2.065(3)
mean Fe−C(5−8)	2.052	2.051	mean Fe−C(9−12)	2.041	2.055
range Fe−C(5−8)	2.041(7)−2.059(7)	2.045(3)−2.059(3)	range Fe−C(9−12)	2.023(7)2.052(7)	2.048(3)−2.064(3)
mean C_{alkyne}−Co(1)	1.959	1.976	C(3)−C(4)	1.462(9)	1.449(4)
mean C_{alkyne}−Co(2)	1.978	1.989	C(13)−C(14)	1.461(8)	1.450(4)
mean C_{alkyne}−Co(3)	1.974	1.969	C(14)−C(15)	1.350(8)	1.342(4)
mean C_{alkyne}−Co(4)	1.980	1.989	C(15)−C(16)	1.494(8)	1.506(4)
C(3)−C(2)−C(1)	140.0(6)	141.0(3)	C(13)−C(14)−C(15)	144.5(6)	144.5(3)
C(2)−C(3)−C(4)	142.9(6)	144.1(3)	C(14)−C(15)−C(16)	143.7(6)	140.3(3)

and angles are given in Table 2. The molecular structure of **7** contains two crystallographically independent molecules within its asymmetric unit. The bond lengths and angles are equivalent within experimental error, and thus discussion will be based upon the average values found within the two residues. One of the most striking features of the solid-state structures of **7** and **11** is that the sulfur atoms are *endodentate*; normally sulfur atoms are situated with their lone pairs *exo* to the macrocyclic cavity unless coordination to a guest ion has occurred.[26] An inspection of the C−S−C−C torsion angles confirms that the sulfur−carbon bonds adopt what is an unusual *anti* conformation (Table 2). This results in the S−C−C−S bonds becoming *gauche* and creating short sulfur···sulfur contacts (3.387 Å in **7** and 3.165, 3.372 Å in **11**). Previous work by Wolf and others suggested that such a contact would be unfavorable due to electron−electron repulsion between the sulfur lone pairs exerting a destabilizing effect on the molecule (the repulsive *gauche* effect).[26,27] The cavity size of **11** may be estimated from the nonbonding S(1)···S(3) separation of 5.848 Å and the Fe(1)···S(2) separation of 5.025 Å.

As might be expected, the long linking chain present in both **7** and **11** causes little distortion of the cyclopentadienyl rings; the rings are virtually parallel with a dihedral angle of 1.8° and 2.5° between the mean planes of the two rings of **7** and **11**, respectively. In contrast to other documented ferrocenophanes,[24] however, the Cp rings are markedly staggered, with a twist angle of 28.9° and 13.4°, respectively. Compound **7** has its cyclopentadienyl rings adopting a 1,2′ disposition with respect to the substituted carbons, with γ being 117°. By contrast, the longer linking chain present in **11** allows the cyclophanes to adopt the more usual 1,3′ disposition ($\gamma = 157.4°$), which is closer to the calculated ideal value of 144°. The solid-state structure of **11** forms a loosely associated dimer (Figure 5) by intermolecular S···H hydrogen bonding [S(1)···H18(C) 2.857 Å; S(1A)···H(18A) 2.857 Å], representing a weak interaction.[28]

To create cyclophanes with a variety of donor functionalities, it was decided to investigate the reactivity of **4** toward 3,6-dithia-1,8-octanediol. Treatment of a dichloromethane solution of **4** with $HOC_2H_4SC_2H_4SC_2H_4OH$ and catalytic amounts of HBF_4 yielded, after separation by preparative TLC, the expected macrocycle [1,1′-Fc{$(Co_2(CO)_6)_2(\mu{:}\eta^2\text{-}\mu{:}\eta^2\text{-}C{\equiv}CCMe_2OC_2H_4SC_2H_4SC_2H_4OCMe_2C{\equiv}C)$}] (**12**) together with [1,1′-Fc{$(Co_2(CO)_6)_2(\mu{:}\eta^2\text{-}\mu{:}\eta^2\text{-}C{\equiv}CC(=CH_2)CH_2CMe_2C{\equiv}C)$}] (**13**), which contains a carbon-only cyclic backbone.

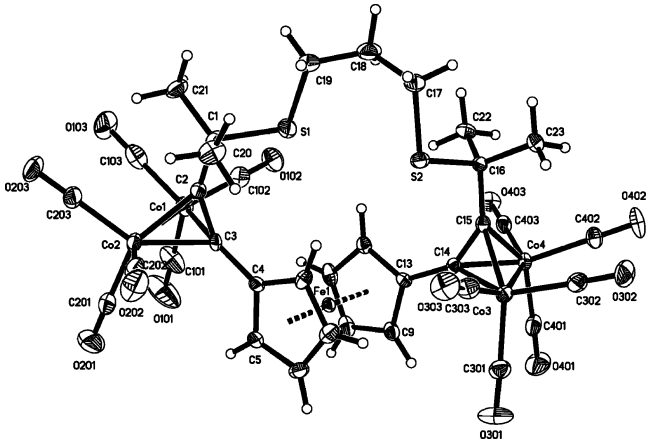

Figure 3. Molecular structure of **7** (ORTEP to 30% probability).

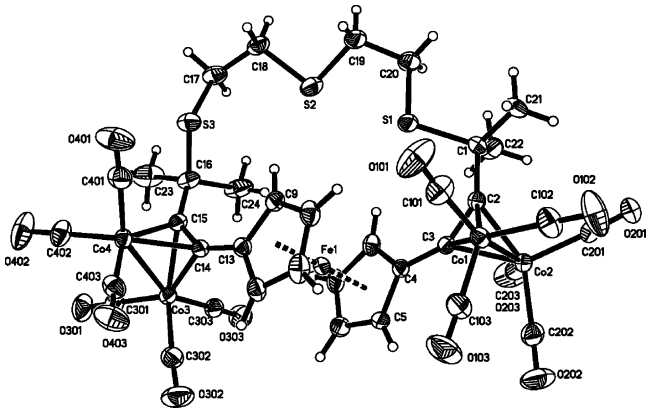

Figure 4. Molecular structure of **11** (30% probability).

The macrocyclic backbone of **12** (Figure 6) contains both O and S atoms that have adopted an *endodentate* conformation. Thus, the average C−S−C−C torsion angle is 179.8° and the average C−O−C−C torsion angle is 174.2°. This leads to short O···S (3.085 Å) and S···S separations (3.249 Å) and again is in marked contrast to reports by Wolf that sulfur atoms adopt an *anti* conformation with respect to each other,[26] although the oxygen atoms do adopt the expected *gauche* conformation.[29] It should be noted that other structurally characterized ferrocenophanes that contain both S and O atoms in their macrocyclic backbone adopt the expected *anti* and *gauche* conformations, respectively.[12,30]

An estimate of the cavity size is given by the nonbonding O1···O1A separation of 7.561 Å and the Fe(1)−

(26) Wolf, R. E.; Hartman, J. R.; Storey, J. M. E.; Foxman, B. M.; Cooper, S. R. *J. Am. Chem. Soc.* **1987**, *109*, 4328.

(27) (a) Zefirov, N. S. *Tetrahedron* **1977**, *33*, 3193. (b) Juaristi, E. *J. Chem. Educ.* **1979**, *56*, 43.

(28) Desiraju, G. R.; Steiner, T. *The Weak Hydrogen Bond in Structural Chemistry and Biology*; Oxford University Press, 1999.

(29) Dale, J. *Tetrahedron* **1974**, *30*, 1683.

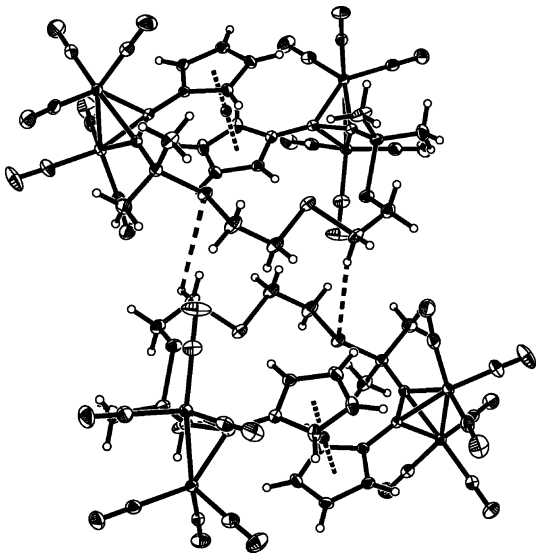

Figure 5. Weak hydrogen-bonding interactions in **11**.

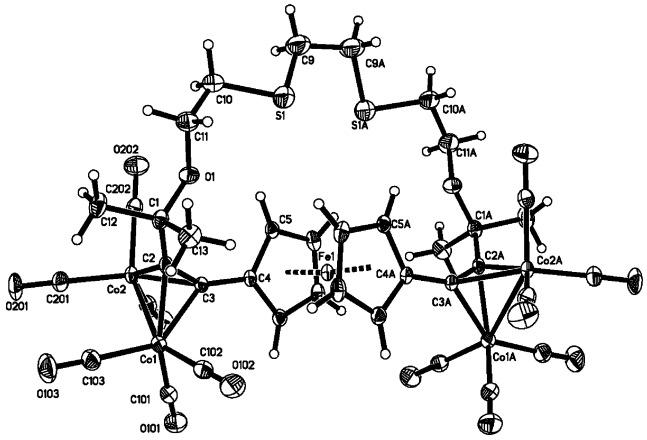

Figure 6. Molecular structure of **12** (ORTEP to 30% probability).

midpoint C(9)−C(9A) separation of 5.804 Å. With regards to the ferrocene unit, the cyclopentadienyl rings are planar (max. deviation 0.002 Å) and are virtually parallel (tilt angle 6.7°). Despite being distinctly staggered (twist = 52.5°), the rings adopt the expected 1,3′ disposition (γ = 163°).

In light of the unexpected conformations of the sulfur atoms in these complexes it was decided to investigate whether any *stabilizing* S···S interactions were present that would account for the *endodentate* conformation. Semiempirical (AM-1) calculations revealed that the HOMO and HOMO−1 (Figure 7) consisted of two essentially orthogonal sulfur lone pairs and that there was a negligible S···S interaction in complex **7**. The orbitals are essentially degenerate (±0.1 eV) and are well isolated from the HOMO−2 (−1 eV) and LUMO (+0.7 eV).

Previous calculations have revealed that the stabilization gained by the sulfur atoms adopting an *anti* configuration in thia-crown compounds is in the region of 1 kcal mol^{-1}, and it should therefore come as little surprise that other factors may override this preference

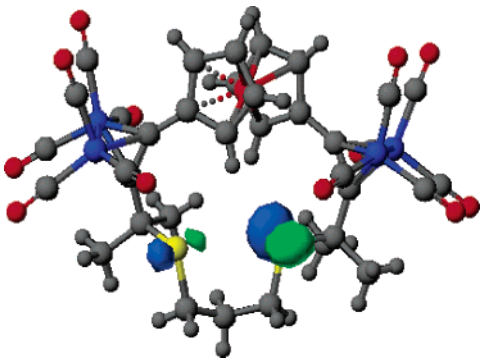

Figure 7. Sulfur-based HOMO and HOMO−1 of **7** (calculated at AM-1 level).

and result in a *gauche* placement of the S−C−C−S bonds.[31] This supposition is supported by the work of Kamigata et al., who reported that all the sulfur atoms in a series of unsaturated thiacrown ethers adopted an *endodentate* conformation.[32] They attributed this *endodentate* conformation to the conformational strain placed upon the system by the *cis*-alkenes present within the backbone. Furthermore, calculations at the RHF/6-31+G* level have shown that the most stable gas phase conformation of thiacrown ethers is up to 5 kcal mol^{-1} more stable than that found in the solid state,[33] thus highlighting the role played by other factors such as packing forces on the solid-state conformation. It is also pertinent at this point to note that the S···Fe separation is always greater than 4 Å (range 4.115−6.432 Å) and that in other documented ferrocene-containing thiacrowns the sulfur atoms are in the expected *exodentate* conformation, thus precluding the possibility of a stabilizing Fe···S interaction.

We therefore attribute the unusual *gauche* conformation of the sulfur atoms in the cyclophanes reported herein to the steric demands placed upon the macrocycle by the cobalt-coordinated alkyne units. The geometry of these units may be compared with some justification to the *cis*-alkenes used in the study by Kamigata and co-workers.

Compound **13** is most probably a result of a competing dehydration−cyclization reaction in which one of the CMe_2OH groups eliminates water to yield intermediate **A** (Scheme 4); the resulting alkene can then attack a carbocation formed by loss of H_2O from the second propargylic site to ultimately yield **13**. We cannot fully rule out the possibility that **13** is formed by a radical-based mechanism similar to that found by Melikyan and co-workers.[34] However, in related studies we have isolated intermediate ene-ynes that could only be formed from a stepwise dehydration of the propargyl alcohols.[35]

It is interesting to note that the related complex [$Co_2(CO)_6(\mu{:}\eta^2$-HC≡$CCMe_2OH$)] reacts with oxygen-based nucleophiles to only yield the expected substitution product, whereas [{$Co_2(CO)_6(\mu{:}\eta^2$-$HOMe_2CC$≡C)−}$_2$]

(30) (a) Bernal, I.; Raabe, E.; Reisner, G. M. *Organometallics* **1988**, *7*, 247. (b) Beer, P. D.; Nation, J. E.; Harman, M. E.; Hursthouse, M. B. *J. Organomet. Chem.* **1992**, *441*, 465. (c) Sato, M.; Anano, H. *J. Organomet. Chem.* **1988**, *555*, 167.

(31) (a) Flory, P. J. *Statistical Mechanics of Chain Molecules*; Interscience: New York, 1969. (b) Oyanagi, K.; Ohta, M.; Sakakibara, M.; Matsuura, H.; Harada, I.; Shimanouchi, T. *Bull. Chim. Soc. Jpn.* **1973**, *46*, 3685.

(32) Tsuchiya, T.; Shimizu, T.; Kamigata, N. *J. Am. Chem. Soc.* **2001**, *123*, 11534.

(33) Hill, S. E.; Feller, D. *J. Phys. Chem. A* **2000**, *104*, 652.

(34) Melikyan, G. G.; Villena, F.; Sepanian, S.; Pulido, M.; Sarkissian, H.; Florut, A. *Org. Lett.* **2003**, *5*, 3395.

(35) Golovko, V. B.; Hope-Weeks, L. J.; Mays M. J.; McPartlin, M.; Sloan, A. M.; Woods, A. D. *New J. Chem.* **2004**, 28, 527.

Scheme 4 . Proposed Pathway Leading to the Formation of 13

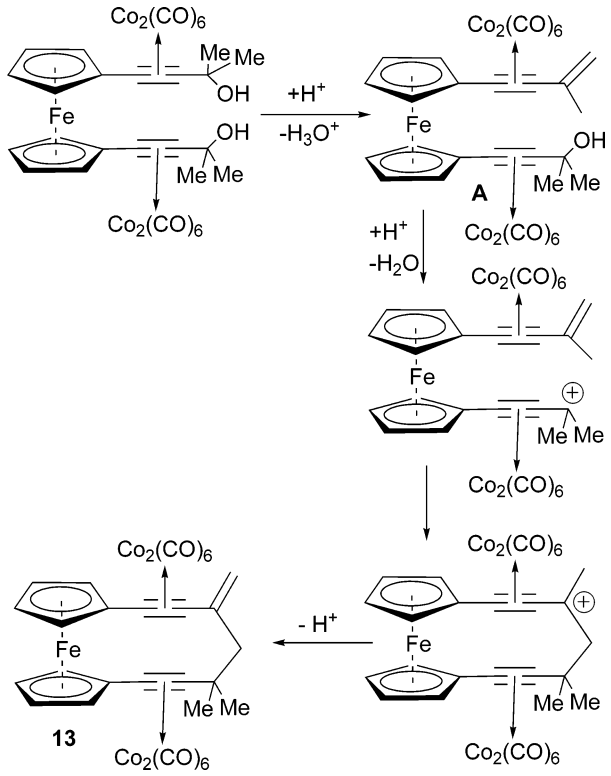

does not react with nucleophiles under any conditions but instead always yields a cyclic product, [{$Co_2(CO)_6$}$_2$-(μ-η^2:μ-η^2-C(=CH_2)C≡C−C≡CCMe_2CH_2)], that contains a bridging motif similar to that found in **13**.[35,36] In further studies it has been shown that only one alkyne of a bis-propargyl alcohol needs to be coordinated in order for dehydration to occur at both sites provided that a direct alkyne−alkyne bond is present.[37] It therefore seems likely that the presence of a second stabilizing group lowers the activation barrier to elimination. This favors dehydration and/or cyclization rather than nucleophilic attack in systems where the cobalt-coordinated alkyne is directly bonded to another group capable of stabilizing a positive charge (e.g., Fc, cobalt-coordinated alkyne).

Elimination reactions at activated propargylic centers are well documented in the case where no nucleophile is present.[38] Thus, compound **13** was synthesized in greater yield by treatment of **4** with an excess of HBF_4 in the absence of nucleophiles. The ^{1}H NMR spectrum of **13** quite clearly indicates that dehydration has occurred; two broad singlets are observed at 5.67 and 5.41 ppm that are assigned as the inequivalent C=CH_2 protons.

The molecular structure of **13** is shown in Figure 8, and relevant bond angles and lengths are shown in Table 4. Regarding the ferrocene unit, the cyclopentadienyl rings are virtually planar (maximum deviation of 0.005 Å) and lie at an angle of 7.1° to each other. The rings are essentially eclipsed (α = 7.62°) and adopt a relative 1,2′ disposition (γ = 65.1°). The complex is

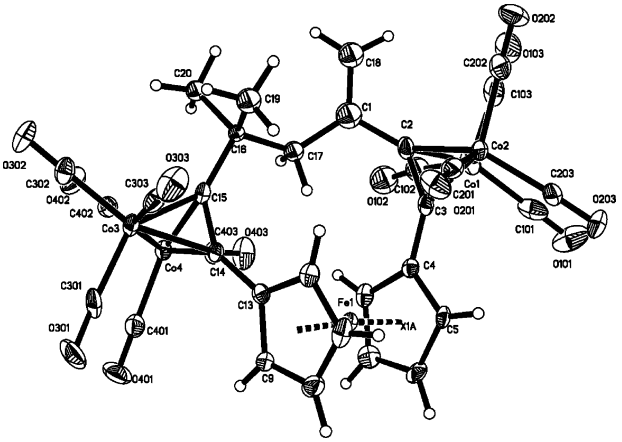

Figure 8. Molecular structure of **13** (ORTEP to 30% probability).

Table 3. Selected Bond Lengths (Å) and Angles (deg) for 12

Fe−C(4)	2.063(7)	Co(1)−C(2)	1.960(3)
mean Fe−C(5−8)	2.052	Co(1)−C(3)	1.961(3)
range Fe−C(5−8)	2.040(3)−2.070(3)	Co(2)−C(2)	1.968(3)
Co(1)−Co(2)	2.4709(6)	Co(2)−C(3)	2.004(3)
C(2)−C(3)	1.339(4)	C(4)−C(3)−C(2)	148.0(3)
C(3)−C(4)	1.445(4)	C(3)−C(2)−C(1)	140.5(3)

disordered about a pseudo-C_2 axis which is located approximately at the Fe atom and midway between the C(1) and C(16) atoms.

It is interesting to note that in all of the structurally characterized complexes presented here except **7** (where the values are identical within experimental error) the alkyne *bend-back angle* is significantly larger at the terminus bound to the cyclopentadienyl ring (average 145.33° compared to 140.44°) (Table 5). Given that the Fc-bound *bend-back* angle is higher in acyclic **4** it seems unlikely that ring strain is the cause for this difference. Higher bend-back angles suggest less donation to the dicobalt unit, and it would therefore make sense that the alkynic carbon bound directly to the ferrocene has the greater bend-back angle due to competition for the alkyne's electron density between the ferrocene and the dicobalt unit.

Electrochemical Studies of the New Complexes. The electrochemical properties of complexes **2**, **4**, **7**, and **11**−**13** were examined by cyclic voltammetry (Figure 9); their redox potentials are shown in Table 5. Coordination of the alkyne to cobalt causes a small cathodic shift in the E_{pa} from 0.80 to 0.78 V. Such a decrease in oxidation potential on dicobalt coordination of alkynyl ferrocenes has also been reported for a series of polyferrocenylalkynes.[39] The variation in the redox potentials for the cyclic compounds appears to follow no discernible pattern (Table 5); certainly it does not correlate to the ring size or number of heteroatoms within the macrocycle. There appears to be no communication between the dicobalt fragment and the ferrocene, as indicated by the two very distinct oxidation potentials. Robinson and co-workers have previously investigated the electronic properties of a series of alkynyl- and dicobaltalkynylferrocenes and have noted that the two redox centers tend to behave independently of each other.[40]

(36) Lockwood, F.; Nicholas, K. M. *Tettrahedron Lett.* **1977**, 4163.
(37) Golovko, V. B.; Mays, M. J.; Woods, A. D. *New J. Chem.* **2002**, *26*, 1706.
(38) Nicholas, K. M. *Acc. Chem. Res.* **1987**, *20*, 207.
(39) Hore, L.-A.; McAdam, C. J.; Kerr, J. L.; Duffy, N. W.; Robinson, B. H.; Simpson, J. *Organometallics* **2000**, *19*, 5039.

Table 4. Selected Bond Lengths (Å) and Angles (deg) for 13

Fe−C(4)	2.091(6)	C(1)−C(17)	1.562(1)
mean Fe−C(5−8)	2.055	C(17)−C(16)	1.48(2)
range Fe−C(5−8)	2.045(7)−2.076(6)	C(15)−C(14)	1.347(9)
Fe−C(13)	2.079(6)	C(2)−C(3)	1.34(1)
mean Fe−C(9−12)	2.052	C(1)−C(2)−C(18)	120(1)
range Fe−C(9−12)	2.047(7)−2.058(6)	C(15)−C(16)−C(19)	106.8(9)
Co(1)−Co(2)	2.464(1)	C(15)−C(16)−C(17)	106(1)
Co(3)−Co(4)	2.464(1)	C(15)−C(16)−C(20)	115.3(1)
mean Co(1)−C_{alkyne}	1.985	C(1)−C(2)−C(3)	142.4(7)
mean Co(2)−C_{alkyne}	1.961	C(2)−C(3)−C(4)	147.2(6)
mean Co(3)−C_{alkyne}	1.982	C(13)−C(14)−C(15)	145.5(6)
mean Co(4)−C_{alkyne}	1.977	C(14)−C(15)−C(16)	137.5(8)
C(1)−C(18)	1.35(2)		

Table 5. Comparison of Geometric Features for the New Complexes

	bend-back angle (deg)		twist angle	γ	ring tilt	atoms in	E_{pa}	E_{pc}	$E_{1/2}$
	Fc	non-Fc	(deg)	(deg)	(deg)	link	(V)	(V)	(V)
2	NA	NA	3.7	3.8	4.1	NA	0.80	0.71	0.76
4	146.0(4)	140.0(5)	30	102.2	1.3	NA	0.78	0.67	0.73
7	142.9(6)	141.0(6)	28.9	117.0	2.5	11	0.77	0.72	0.75
	144.5(6)	143.7							
11	144.1(3)	141.0(3)	13.4	157.4	6.7	13	0.85	0.67	0.76
	144.5(3)	140.3(3)							
12	148.0(3)	140.5(3)	52.5	163	7.1	16	0.79	0.63	0.71
13	147.2(6)	138.8(8)	7.6	65.1	4.1	7	0.85	0.73	0.79
	145.4(6)	138.2(7)							
av	145.33	140.44							

At standard scan rates (ca. 100 mV s^{-1}) all the complexes exhibit quasi-reversible electrochemical behavior. The voltammogram displays a catalytic current profile at scan rates less than 3 mV s^{-1} for **2** and 20 mV s^{-1} for **4**, indicative of an ECE′ mechanism (Figure 10). The rate of this chemical reaction is only competitive with the electrochemical process at slower scan rates, but it is interesting to note that the rate appears to increase upon complexation with $Co_2(CO)_6$, suggesting that the chemical reaction may be centered at the propargyl unit, which is further activated by complexation with $Co_2(CO)_6$. To the best of the authors' knowledge there has been no research into the electrochemical behavior of cobalt-coordinated propargyl alcohols, although it is known that propargyl cations can undergo a one-electron reduction on treatment with zinc to form radical species.[41] Furthermore, Melikyan has observed that electron transfer between a $Co_2(CO)_6$ center and a propargyl cation can occur prior to a radical coupling reaction, and it seems likely that a similar transfer between ferrocene and the propargyl center is occurring in the present case.[34]

To explore this reaction more, it was decided to carry out the bulk oxidation of a sample of **2**. Treatment of an acetone solution of **2** with 0.5 equiv of ammonical cerium(IV) nitrate resulted in an immediate color change from orange to green. However, after stirring for several minutes a second color change from green to deep orange occurred, suggesting a chemical reduction of **2**. Unfortunately, despite repeated efforts we have not been able to separate the products of this reaction.

(40) (a) McAdam, C. J.; Kerr, J. L.; Duffy, N. W.; Robinson, B. H.; Simpson, J. *Organometallics* **1996**, *15*, 3935. (b) McAdam, C. J.; Brunton, J. L.; Robinson, B. H.; Simpson, J. *J. Chem. Soc., Dalton Trans.* **1999**, 2487.

(41) Melikyan, G. G.; Khan, M. A.; Nicholas, K. M. *Organometallics* **1995**, *14*, 2170.

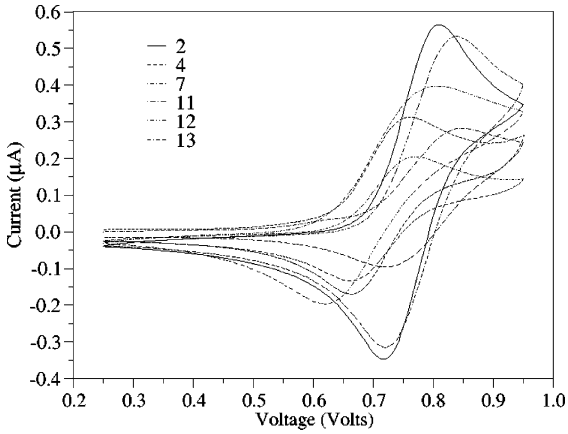

Figure 9. Cyclic voltammograms of the new complexes (ν = 100 ms^{-1}).

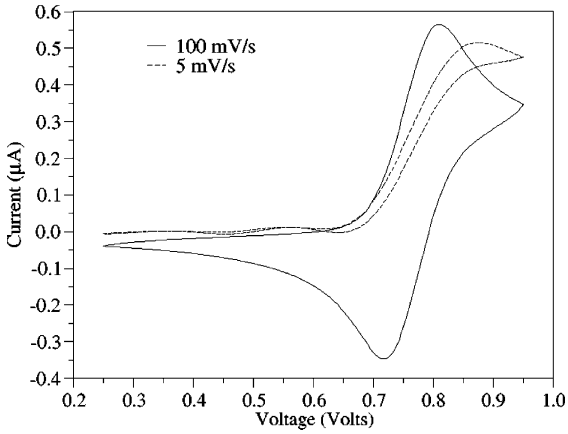

Figure 10. Cyclic voltammograms of **2** at varying scan rates.

Conclusions

A facile one-pot synthesis of a new range of alkynylferrocene-containing macrocycles is reported; in all cases only monomeric products were formed. The presence of the dicobalt-coordinated alkyne results in both the oxygen and sulfur heteroatoms being located with their lone pairs *endodentate*. The electrochemical properties of the new complexes have been investigated; these show quasi-reversible behavior at high scan rates, but oxidation of **2** and **4** becomes irreversible at slow (<20 mV s^{-1}) scan rates, presumably due to a chemical reaction involving the propargyl centers.

Experimental Section

Unless otherwise stated all experiments were carried out under an atmosphere of dry, oxygen-free nitrogen, using

Table 6. X-ray Crystallographic Data for the New Complexes[a]

	2	**4**	**7**	**11**	**12**	**13**
empirical formula	$C_{20}H_{22}FeO_2$	$C_{32}H_{22}Co_4O_{14}$	$C_{35}H_{26}Co_4O_{12}S_2$	$C_{36}H_{28}Co_4O_{12}S_3$	$C_{38}H_{32}Co_4FeO_{14}S_2$	$C_{32}H_{18}Co_4FeO_{12}$
weight	350.23	922.07	994.25	1040.33	1068.33	886.03
cryst syst	monoclinic	orthorhombic	monoclinic	monoclinic	monoclinic	monoclinic
cryst size	0.32 × 0.10 × 0.10	0.16 × 0.14 × 0.12	0.23 × 0.18 × 0.02	0.28 × 0.23 × 0.12	0.35 × 0.32 × 0.12	0.46 × 0.28 × 0.05
space group	*P*2(1)/*c*	*P*1	*P*2(1)/*c*	*P*(2)1/*c*	*P*2/*c*	*P*2(1)/*n*
a (Å)	14.2647(4)	12.3936(3)	12.4781(2)	8.1828(1)	14.4980(5)	8.4267(1)
b (Å)	10.9838(3)	10.4536(2)	22.3700(3)	34.1578(3)	10.8391(3)	30.2975(4)
c (Å)	10.6930(2)	26.6811(5)	27.1757(4)	14.6109(1)	14.0975(4)	13.4300(2)
α (deg)	90	90	90	90	90	90
β (deg)	90.252(1)	90	90.0790	102.049(1)	108.514(1)	106.568(1)
γ (deg)	90	90	90	90	90	90
V (Å^3)	1675.37(7)	3456.7(1)	7585.68(19)	3993.87(7)	2100.7(11)	3286.43(8)
Z	4	4	8	4	2	4
D_c (Mg/m^3)	1.389	1.772	1.741	1.730	1.689	1.791
abs coeff (mm^{-1})	0.907	2.357	2.257	2.198	2.048	2.471
F(000)	736	1840	3984	2088	1076	1760
θ range (deg)	3.71 to 27.42	3.63 ro 20.62	3.52 to 27.16	1.19 to 27.49	3.58 to 27.50	3.60 to 27.49
index ranges	$-12 \le h \le 18$ $-14 \le k \le 14$ $-13 \le l \le 13$	$-12 \le h \le 12$ $-7 \le k \le 10$ $-26 \le l \le 26$	$-15 \le h \le 15$ $-28 \le k \le 28$ $-34 \le l \le 34$	$-10 \le h \le 10$ $-44 \le k \le 44$ $-15 \le l \le 18$	$-18 \le h \le 18$ $-14 \le k \le 13$ $-18 \le l \le 18$	$-10 \le h \le 10$ $-39 \le k \le 39$ $-17 \le l \le 17$
reflns no. of measd	10 581	13 109	53 199	30 802	12 057	22 450
no. of indep reflns	3809	1753	15 988	8847	4785	7212
R_{int}	0.0477	0.0974	0.0701	0.0387	0.0333	0.1202
goodness of fit on F^2	1.031	1.202	1.091	1.257	1.064	1.037
final *R* indices R1	0.0371	0.0327	0.0659	0.0297	0.0413	0.0626
wR2	0.0812	0.0900	0.1444	0.0963	0.1088	0.1599
R indices (all data) R1	0.0524	0.0384	0.0950	0.0452	0.0494	0.0973
wR2	0.0882	0.1067	0.1610	0.1330	0.1150	0.2038
largest diff peak and hole (e/Å^3)	0.416 and −0.478	0.496 and −0.603	2.192 and −1.231	0.827 and −1.505	1.697 and −1.084	0.904 and −1.179

[a] Data collected at 180(2) K.

conventional Schlenk line techniques, and solvents freshly distilled from the appropriate drying agent. Except where otherwise indicated NMR spectra were recorded in $CDCl_3$ using a Bruker DRX 400 spectrometer, with TMS as an external standard for ^{1}H and ^{13}C spectra and H_3PO_4 as an external standard for ^{31}P NMR spectra. Infrared spectra were, unless otherwise stated, recorded in dichloromethane solution in 0.5 mm NaCl solution cells, using a Perkin-Elmer 1710 Fourier transform spectrometer. FAB mass spectra were obtained using a Kratos MS 890 instrument, using 3-nitrobenzyl alcohol as a matrix. Preparative TLC was carried out on 1 mm silica plates prepared at the University of Cambridge. Column chromatography was performed on Kieselgel 60 (70−230 mesh ASTM). All products are listed in order of decreasing R_f. Unless otherwise stated, all reagents were obtained from commercial suppliers and used without further purification. Diiodoferrocene was prepared by the literature method.[42]

Crystal Structure Determinations. Single-crystal X-ray diffraction data were collected using a Nonius-Kappa CCD diffractometer, equipped with an Oxford Cryosystems cryostream and employing Mo Kα (0.71069 Å) irradiation from a sealed tube X-ray source. Cell refinement, data collection, and data reduction were performed with the programs DENZO and COLLECT, and multiscan absorption corrections were applied to all intensity data with the program SORTAV. All structures were solved and refined with the programs SHELXS97 and SHELXL97, respectively.[43−46] The structure of complex **13** shows disorder about a pseudo-C_2 axis located approximately between the Fe(1) atom and the midpoint of the C(16)−C(1) atoms of the carbacyclic ring. This leads to two positions of the C(1), and C(16) to C(20) atoms being observed in an approximately 2:1 ratio. The two positions were refined with the total occupancy of the site summing to unity. A summary of data collection and data refinement details is given in Table 6.

Electrochemical Studies. Cyclic voltammetric studies were carried out using tetra(*tert*-butyl)ammonium tetrafluoroborate as the electrolyte (0.1 M) and dichloromethane as the solvent. A standard Ag/AgCl electrode was used as the reference electrode, along with platinum working and auxiliary electrodes. The scan rate was 100 mV s^{-1}. Each voltammogram shows linear plots of I_p^a versus $v^{1/2}$.

Theoretical Calculations. Semiempirical RHF calculations were made using MOPAC, implemented through Quantum Cache (Fujitsu Co.) utilizing the crystallographic geometry.[47] Semiempirical calculations on transition metal complexes at this level are hindered by a shortage of appropriate basis sets. However, the Austin Model 1 (AM1) is parameterized for Fe,[48] but not Co, and so the bonding in **7** was probed using the isoelectronic Fe complex in which Co atoms were replaced by Fe^- ions.

Synthesis of [1,1′-Fc(C≡CCH$_2$OH)I] (1) and [1,1′-Fc(C≡CCMe$_2$OH)$_2$] (2). To a solution of 1,1′-FcI_2 (5.2 g, 12 mmol) in ^{i}Pr$_2$NH (200 mL) were added $Cu(OAc)_2$ (0.09 g, 4 mol %) and $Pd(PPh_3)_2Cl_2$ (0.34 g, 4 mol %), and the resulting mixture was stirred for 30 min. The relevant propargyl alcohol (3 equiv) was added, and the solution was heated under reflux overnight. The solvent was removed in vacuo, and the residue was dissolved in the minimum dichloromethane, absorbed on silica, and applied to the top of a silica column.

(42) Kovar, R. F.; Raush, M. D.; Rosenberg, H. *Organomet. Chem. Synth.* **1970/1971**, *1*, 173.
(43) Otwinowski, Z.; Minor, W. *Methods Enzymol*. **1997**, *276*, 307.
(44) Hooft, R. *COLLECT*; Nonius BV: Delft, The Netherlands, 1998.
(45) Blessing, R. H. *Acta Crystallogr.* **1995**, *A51*, 33.
(46) Sheldrick, G. M. *SHELXS97* and *SHELXL97*; University of Göttingen: Germany.
(47) *Quantum Cache* vers. 5.0; Fujitsu Co.: Japan, 2001.
(48) Parameters for C, H, and O are published in: Dewar, M. J. S.; Zoebisch, E. G.; Healy, E. F.; Stewart J. J. P. *J. Am. Chem. Soc.* **1985**, *107*, 3902. For S, see: Dewar, M. J. S.; Yuan, Y.-C. *Inorg. Chem.* **1990**, *29*, 3881. Parametrization of Fe, see: Voityuk, A. A. Unpublished, MOPAC implemented in ref 47.

Data for 1. Elution with hexane/ethyl acetate (3:2) yielded [1,1′-Fc(C≡CCH$_2$OH)I] (**1**) as a yellow oil (2.66 g, 61%). ^{1}H NMR δ: 4.41 (s, 2H, C*H*$_2$OH), 4.40 (t, 2H, Cp, $^3J_{H-H}$ = 1.9 Hz), 4.38 (t, 2H, Cp, J_{H-H} = 1.9 Hz), 4.20 (t, 2H, Cp, J_{H-H} = 1.9 Hz), 4.19 (t, 2H, Cp, J_{H-H} = 2.0 Hz). ^{13}C NMR δ: 86.1 (Cp, C−C) 84.9, 83.3 (C≡C), 76.2, 74.1, 71.9, 70.9 (Cp, *C*H), 66.7 (Cp, C−C), 53.09 (CH$_2$OH), 41.0 (Cp, C). FABm/s: 366 (MH$^+$). Anal. Calcd for $C_{13}FeH_{11}IO$: C 42.66, H 3.03. Found: C 43.28, H 3.05.

Data for 2. Elution with hexane/ethyl acetate (1:1) yielded orange crystalline **2** (2.48, 70%). Spectra were in accordance with the literature values.

Synthesis of [1,1′-Fc{Co$_2$(CO)$_6$(μ-η^2-C≡CCH$_2$OH)}I] (3) and [1,1′-Fc{Co$_2$(CO)$_6$(μ-η^2-C≡CCMe$_2$OH)}$_2$] (4). To a solution of **1** or **2** (5 mmol) in toluene (250 mL) was added Co$_2$(CO)$_8$ (2.05 g, 6 mmol for **1**; 4.1 g, 12 mmol for **2**), and the mixture was stirred at room temperature for 3 h. The solvent was removed on a rotary evaporator, and the residue was dissolved in the minimum volume of dichloromethane and applied to the top of a silica chromatography column. Elution with hexane/ethyl acetate (1:1) followed by removal of solvent yielded green crystalline **3** (1.43 g, 44%) or **4** (2.76 g, 60%).

Data for 3. IR νCO (cm^{-1}): 2076.1(s), 2052.4(vs), 2022.6(vs). ^{1}H NMR δ: 5.04 (d, 2H, C*H*$_2$OH, $^3J_{H-H}$ = 6.1 Hz), 4.40 (t, 2H, Cp, $^3J_{H-H}$ = 1.8 Hz), 4.37 (t, 2H, Cp, $^3J_{H-H}$ = 1.9 Hz), 4.30 (t, 2H, Cp, $^3J_{H-H}$ = 1.8 Hz), 4.20 (t, 2H, Cp, $^3J_{H-H}$ = 1.9 Hz). ^{13}C NMR δ: 199.3 (CO), 97.1, 89.7, (C≡C), 86.2 (Cp, C−C), 75.9, 72.9, 72.8, 70.6 (Cp, CH), 66.75 (Cp CC), 63.90 (CH$_2$OH). FABm/s: 652 (MH$^+$), MH$^+$ − *n*CO (*n* = 2−5). Anal. Calcd for $C_{19}Co_2FeH_{11}IO_7$: C 35.00, H 1.70. Found: C 33.29, H 1.92.

Data for 4. IR νCO (cm^{-1}): 2079.6(s), 2050.2(vs), 2023.0(vs). ^{1}H NMR δ: 4.47 (s, 2H, CpH), 4.44 (s, 2H, CpH), 1.74 (s, 6H, Me). ^{13}C NMR δ: 199.6 (s, *C*O), 107.2 (s, *C*≡C), 89.96 (s, C≡*C*), 86.28 (s, Cp, C−C), 73.19 (s, *C*Me$_2$), 72.30, 70.63 (s, CpH), 32.66 (s, *C*H$_3$). FABm/s: 922.6 (MH$^+$), 921.6 (M$^+$), M$^+$ − *n*CO (*n* = 3−8). Anal. Calcd for $C_{32}H_{22}Co_4FeO_{14}$: C 41.68, H 2.40. Found: C 41.54, H 2.36.

Preparation of [1,1′-Fc{Co$_2$(CO)$_4$(dppm)(μ-η^2-C≡CCH$_2$OH)}I], 6. To a solution of **3** (2.0 g, 3.07 mmol) in toluene (200 mL) was added dppm (1.84 g, 4.80 mmol) and the mixture heated to 70 °C and stirred for 2 h. The solvent was removed on a rotary evaporator, and the residue was dissolved in the minimum volume of dichloromethane and applied to the top of a silica chromatography column. Elution with 4:1 hexane/ethyl acetate yielded [1,1′-Fc{Co$_2$(CO)$_4$(dppm)(μ-η^2-C≡CCH$_2$OH)}I] (**6**) as a red solid (2.58 g, 86%). IR νCO (cm^{-1}): 2020.1(s), 1992.0(vs), 1964.7(s). ^{1}H NMR δ: 7.36−7.18 (m, 20H, Ph), 5.10 (br s, 2H, CH$_2$OH), 4.42 (t, 2H, Cp, J_{H-H} = 1.8 Hz), 4.28 (t, 2H, Cp, J_{H-H} = 1.8 Hz), 4.26 (t, 2H, Cp, J_{H-H} = 1.8 Hz), 4.21 (t, 2H, Cp, J_{H-H} = 1.8 Hz), 3.74 (m, PC*H*HP, 1H), 3.50 (m, PCH*H*P). ^{13}C NMR δ: 204.8 (s, *C*O), 131.6 (m, Ph), 129.5 (d, Ph, J_{C-P} = 30 Hz), 128.2 (d, Ph, J_{C-P} = 15 Hz), 91.4 (C≡C), 88.61 (C≡*C*), 84.80 (Cp, C−C), 75.2, 72.5, 71.8, 70.5 (Cp, H), 69.01 (s, Cp, C−C), 65.9 (*C*H$_2$OH), 40.2 (t, P*C*H$_2$P, J_{C-P} = 76 Hz). ^{31}P NMR δ: 38.5 (s). FABm/s: 981 (M$^+$), M$^+$ − *n*CO (*n* = 1−4). Anal. Calcd for $C_{42}H_{22}Co_2FeIO_5P_2$: C 51.5, H 3.4, P 6.3. Found: C 52.1, H 3.67, P 4.76.

General Methodology for Reaction with Thiols. To a solution of **3** or **4** (0.20 mmol) in DCM (50 cm^3) were added 54 wt % HBF$_4$·OEt$_2$ (0.05 mL, 0.0034 mmol) at −78 °C and the appropriate dithiol HSZSH (0.24 mmol, 1.2 equiv). The resultant mixture was stirred for 10 min at −78 °C, then allowed to warm to RT and stirred for a further 2 h. The reaction was quenched with an excess of NaHCO$_3$ and dried with MgSO$_4$. The mixture was filtered through a silica plug, the solvent removed in vacuo, and the residue redissolved in the minimum DCM and applied to the base of TLC plates. The reaction products were separated as follows.

Data for 5. Elution with 4:1 hexane/ethyl acetate yielded two major fractions, but decomposition led to isolation of only the green solid [1,1′-Fc{Co$_2$(CO)$_6$(μ:η^2-C≡CCH$_2$SCH$_2$CH$_2$OCH$_2$CH$_2$SH)}I] (**5**) (0.03 mmol, 14%). IR νCO (cm^{-1}): 2079.5(s), 2048.0(vs), 2018.6(vs). ^{1}H NMR δ: 4.45 (t, 2H, Cp, J_{H-H} = 1.5 Hz), 4.42 (t, 2H, Cp, J_{H-H} = 1.5 Hz), 4.35 (t, 2H, Cp, J_{H-H} = 1.6 Hz), 4.29 (s, 2H, C$_2$C*H*$_2$S), 4.25 (t, 2H, Cp, J_{H-H} = 1.5 Hz), 3.80 (t, 2H, C*H*$_2$O, J_{H-H} = 6.4 Hz), 3.78 (t, 2H, C*H*$_2$O, J_{H-H} = 6.4 Hz), 2.97 (t, 2H, CH$_2$S, J_{H-H} = 6.4 Hz), 2.91 (t, 2H, CH$_2$S, J_{H-H} = 6.4 Hz). ^{13}C NMR δ: 89.9, 86.4 (C≡C), 75.8, 73.3, 72.5 (Cp, CH), 71.5 (Cp, C−C), 70.9 (Cp, CH), 69.4 (Cp, C−C), 53.4 (C$_2$CH$_2$S), 38.6, 37.8, 33.3, 29.7 (CH$_2$).

Data for [1,1′-Fc{(Co$_2$(CO)$_6$)$_2$(μ:η^2-μ:η^2-C≡CCMe$_2$S(CH$_2$)$_3$SCMe$_2$C≡C)}], 7. IR νCO (cm^{-1}): 2082.4(s), 2049.0(vs), 2019.0(s). ^{1}H NMR δ: 4.59 (s, 4H, Cp), 4.17 (s, 4H, Cp), 2.93 (m, 4H, Me$_2$CSC*H*$_2$), 2.19 (m, 2H, SCH$_2$C*H*$_2$), 1.76 (s, 12H, C*H*$_3$). ^{13}C NMR δ: 199.78 (s, *C*O), 106.5 (*C*≡C), 91.12 (s, C≡*C*), 86.85 (s, CpCC), 74.77, 73.57 (s, CpCH), 48.57 (s, *C*Me$_2$), 31.57 (*C*H$_3$), 29.51 (s, SCH$_2$), 29.18 (s, SCH$_2$*C*H$_2$). FABm/s: 993.7 (MH$^+$), M$^+$ − *n*CO (*n* = 2,4, 6−10). Anal. Calcd for $C_{35}H_{26}Co_4FeO_{12}S_2$: C 42.28, H 2.64. Found: C 43.06, H 2.12.

Data for [1,1′-Fc{(Co$_2$(CO)$_6$)$_2$(μ:η^2-μ:η^2-C≡CCMe$_2$S(CH$_2$)$_4$SCMe$_2$C≡C)}], 8. IR νCO (cm^{-1}): 2083.3(m), 2054.2(s), 2022.6(s). ^{1}H NMR δ: 4.61 (t, $^3J_{H-H}$ = 1.8 Hz, 4H, Cp), 4.22 (t, $^3J_{H-H}$ = 1.8 Hz, 4H, Cp), 2.20 (m, 4H, C*H*$_2$S), 1.75 (s, 12H, Me), 1.15 (m, 4H, C*H*$_2$). ^{13}C NMR δ: 199.5 (br, *C*O), 105.8 (*C*≡C), 90.89 (C≡*C*), 85.89 (s, Cp, C−C), 74.12, 72.78 (s, Cp, CH), 48.71 (*C*Me$_2$), 33.10 (S*C*H$_2$CH$_2$), 32.80 (*C*H$_3$) 30.6 (*C*H$_2$). FABm/s: 1008 (MH$^+$), M$^+$ − *n*CO (*n* = 1−4). Anal. Calcd for $C_{36}H_{28}Co_4FeO_{12}S_2$: C 42.88, H 2.80. Found: C 42.96, H 3.10.

Data for [1,1′-Fc{(Co$_2$(CO)$_6$)$_2$(μ:η^2-μ:η^2-C≡CCMe$_2$S(CH$_2$)$_5$SCMe$_2$C≡C)}], 9. IR νCO (cm^{-1}): 2085.3(m), 2050.2(s), 2020.6(s). ^{1}H NMR δ: 4.58 (t, $^3J_{H-H}$ = 1.8 Hz, 4H, Cp), 4.26 (t, $^3J_{H-H}$ = 1.8 Hz, 4H, Cp), 2.26 (m, 4H, C*H*$_2$S), 1.81 (s, 12H, C*H*$_3$), 1.18 (m, 4H, C*H*$_2$), 1.16 (m, 2H, C*H*$_2$). ^{13}C NMR δ: 199.5 (br, *C*O), 108.8, 94.5 (C≡C), 86.12 (s, Cp, *C*−C), 74.12, 71.26 (s, Cp, CH), 48.7 (*C*Me$_2$), 33.14 (SCH$_2$*C*H$_2$), 32.62 (*C*H$_3$), 30.6 (*C*H$_2$), 28.0 (*C*H$_2$). FABm/s: 1022 (MH$^+$), M$^+$ − *n*CO (*n* = 1−4, 6, 8−10). Anal. Calcd for $C_{37}H_{30}Co_4FeO_{12}S_2$: C 43.47, H 2.96. Found: C 43.48, H 3.10.

Data for [1,1′-Fc{(Co$_2$(CO)$_6$)$_2$(μ:η^2-μ:η^2-C≡CCMe$_2$S(CH$_2$)$_6$SCMe$_2$C≡C)}], 10. IR νCO (cm^{-1}): 2086.4(m), 2051.4(s), 2021.4(s). ^{1}H NMR δ: 4.55 (t, $^3J_{H-H}$ = 1.8 Hz, 4H, Cp), 4.21 (t, $^3J_{H-H}$ = 1.8 Hz, 4H, Cp), 2.7 (m, 8H, CH$_2$S), 2.25 (m 4H, CH$_2$S), 1.8 (s, 12H, CH$_3$). ^{13}C NMR δ: 200.0 (s, CO), 106.6 (*C*≡C), 94.0 (C≡*C*), 86.12 (s, Cp, *C*−C), 74.12, 71.26 (s, CpC−H), 49.2 (C≡C*C*Me$_2$S), 38.9 (SCH$_2$), 31.0 (C*C*H$_3$), 28 (br, CH$_2$). FABm/s: 1037 (MH$^+$), M$^+$ − *n*CO (*n* = 1, 3−10, 12). Anal. Calcd for $C_{38}H_{32}Co_4FeO_{12}S_2$: C 44.04 H 3.11. Found: C 45.18, H 4.02.

[1,1′-Fc{(Co$_2$(CO)$_6$)$_2$(μ:η^2-μ:η^2-C≡CCMe$_2$SC$_2$H$_4$SC$_2$H$_4$SCMe$_2$C≡C)}], 11. IR νCO (cm^{-1}): 2084(s), 2049(vs), 2021(vs). ^{1}H NMR δ: 4.29 (s, v br, 8H, Cp); 3.09 (d, $^3J_{H-H}$ 6.1 Hz, 4H, SC*H*$_2$), 3.04 (d, $^3J_{H-H}$ = 6.1 Hz, 4H, SCH$_2$C*H*$_2$S), 1.80(s, 12H, Me). ^{13}C NMR δ: 199.80 (s, *C*O), 96.12 (s, *C*≡C), 84.16 (s, C≡*C*), 82.32 (s, Cp, C−C), 74.38 (s, Cp, CH), 70.14 (s, *C*Me$_2$), 69.65 (s, Cp, CH), 32.80 (s, CH$_2$), 31.98 (s, CH$_2$), 31.55 (s, CH$_3$). FABm/s: 1040.2 (M$^+$), M$^+$ − *n*CO (*n* = 2−10). Anal. Calcd for $C_{36}H_{28}Co_4FeO_{12}S_3$: C 41.56, H 2.71. Found: C 41.44, H 2.98.

[1,1′-Fc{(Co$_2$(CO)$_6$)$_2$(μ:η^2-μ:η^2-C≡CCMe$_2$OC$_2$H$_4$SC$_2$H$_4$SC$_2$H$_4$OCMe$_2$C≡C)}], 12. IR νCO (cm^{-1}): 2085(s), 2050(vs), 2020(vs). ^{1}H NMR δ: 4.58 (t, $^3J_{H-H}$ 1.8 Hz, 4H, Cp*H*), 4.46 (t, $^3J_{H-H}$ 1.8 Hz, 4H, Cp*H*), 3.68 (t, $^3J_{H-H}$ 7.2 Hz, 4H, OC*H*$_2$), 2.77 (s, 4H, SC*H*$_2$), 2.75 (t, $^3J_{H-H}$ 7.2 Hz, 4H, OCH$_2$C*H*$_2$), 1.67 (s, 12H, C*H*$_3$). ^{13}C NMR δ: 199.78 (s, *C*O), 106.131 (s, *C*≡C), 91.57 (s, C≡*C*), 86.28 (s, Cp, C−C), 72.27 (s, Cp, CH), 71.46 (s, Cp, CH), 63.09 (s, O*C*H$_2$), 33.04 (s, *C*H$_2$S), 32.52 (s, S*C*H$_2$), 27.53 (s, *C*H$_3$). FABm/s: 1068.3 (M$^+$), M$^+$ − *n*CO (*n* = 3, 6−10). Anal. Calcd for $C_{38}H_{32}Co_4FeO_{14}S_2$: C 42.72, H 3.02. Found: C 43.07, H 2.12.

Data for [1,1′-Fc{(Co$_2$(CO)$_6$}$_2$(μ:η^2-μ:η^2-C≡CC(=CH$_2$)CH$_2$CMe$_2$C≡C)}], 13. IR νCO (cm^{-1}): 2083(s), 2050(vs), 2023(vs). ^{1}H NMR δ: 5.67 (s, br, 1H, C=C*H*H), 5.41 (s, br, 1H, C=CH*H*), 4.43 (t, $^3J_{H-H}$ 1.9 Hz, 4H, Cp*H*), 4.41 (t, $^3J_{H-H}$ 1.9 Hz,

4H, Cp*H*), 2.27 (s, 6H, Me), 1.66 (s, 2H, CH_2). ^{13}C NMR δ: 199.48, 145.22 (s, *C*=CH_2), 121.78 (s, C=*C*H_2), 106.31 (s, *C*≡C), 90.46 (s, C≡*C*), 87.68 (s, Cp, C−C), 72.41 (s, Cp, CH), 69.46 (s, Cp, CH), 47.33 (s, *C*Me_2), 40.06 (s, *C*H_2), 31.38 (s, Me). FABm/s: 887 (MH^+), 886 (M^+), $M^+ - n$CO (n = 1−11). Anal. Calcd for $C_{32}H_{18}Co_4FeO_{12}$: C 43.38, H 2.05. Found: C 43.05, H 2.05.

Acknowledgment. We acknowledge the financial support of the EPSRC for the purchase of the Nonius Kappa CCD diffractometer and the help of the EPSRC mass spectrometry service, Swansea. A.D.W. is grateful to St. Catharine's College, Cambridge, for the award of a Research Fellowship. We thank the Cambridge Overseas Trust for financial support to V.B.G. C.M.H. would like to acknowledge support from NPL's Strategic Research Programme. Dr. John E. Davies is thanked for help with data collection and crystal structure determination.

Supporting Information Available: This material is available free of charge via the Internet at http://pubs.acs.org.

OM049465E